FULL PAPER

The Stone Age Revisited: Building a Monolithic Inorganic Lithium-Ion Battery

Gaelle Delaizir, Virginie Viallet, Abdelmaula Aboulaich, Renaud Bouchet, Laurence Tortet, Vincent Seznec, Mathieu Morcrette, Jean-Marie Tarascon, Patrick Rozier, and Mickael Dollé*

A new path for the design of safe and efficient, all-solid-state Li-ion batteries by spark plasma sintering (SPS) is considered. To reach a good electrochemical performance from such batteries, several parameters are investigated, such as the composite-electrode formulation (active material/electrolyte/carbon ratio) and the influence of the sintering parameters on their compactness. The formulation is optimized to ensure good ionic and electronic percolation through the composite electrode's volume. The compactness has to be sufficient to guarantee a good mechanical aspect, while the residual porosity in the composite electrode allows electrode-volume changes upon insertion and deinsertion, preserving the electrode/electrolyte interfaces, which are crucial in such technology. Based on these investigations, an all-solid-state battery with a surface capacity of 2.2 mA h cm^{-2} is assembled by SPS, displaying a promising electrochemical performance at 80 °C.

1. Introduction

Lithium-ion batteries are the focus of much research around the world, due to their high volumetric and gravimetric energy density. This technology has conquered the market of lightweight electronic devices such as lap-top computers, cellular phones and personal digital assistants (PDAs). However, safety and cost are the main concerns to their application in the potential mass market of electric vehicles and other particular applications that require a high temperature (oil drilling and military applications). The most important safety issue deals with the inherent instability of the liquid electrolyte, which requires the development of a non-flammable electrolyte with a high ionic conductivity (>10^{-3} S cm^{-1}).[1,2] Solid-state electrolytes, such as polymer electrolytes or ceramic electrolytes, are perfect answers to this safety issue.[3]

For inorganic, all-solid-state batteries, considerable effort has been devoted to the development of microbatteries for their application in microelectronics.[4] These batteries, which consist of a stack of three, thin, dense components, namely a positive electrode, a solid electrolyte and a negative electrode, are fabricated using expensive, multistep processes based on thin-layer-deposition techniques, such as chemical vapour deposition,[5] RF-sputtering[6–8] or pulsed vapor deposition. [9,10] Typically, these microbatteries have a total thickness around 15 μm including the protective packaging, and their specific capacities lie between 5 and 100 μA h cm^{-2}, depending on the thickness of the electrodes.[11] Increasing the thickness of the electrodes further has been a long-lasting dream that has failed so far because of the formation of microcracks between the components, due to stress generated at the solid/solid interfaces due to the volume change of the active material during cycling. Furthermore, strong kinetic limitations have been observed when an upscale in the third dimension is done, due to the low mobilities of the ions/electrons in solid-state active materials.[4] The main challenge facing all-inorganic Li-ion batteries is the increase of the stored capacity per square centimeter[2] (i.e., the thickness of the electrode). It is a sizeable challenge to combine the advantages of all-solid-state batteries (safety, mechanical integrity, etc) and the large volumetric and gravimetric energy density of lithium-ion batteries.

A solution lies in the use of composite electrodes, which are made from a multifunctional material: they should present a high content of an electrochemically active material to get a high energy density, as well as contain electronic- and ionic conductor additives to ensure efficient and homogeneous transfer of electrons and ions in the electrode volume. Composite electrodes should also display a good mechanical aspect to allow easy handling and to ensure cell lifetime. The main difficulty is

Dr. G. Delaizir, Dr. P. Rozier, Dr. M. Dollé
Centre d'Elaboration de Matériaux et d'Etudes Structurales-CNRS
UPR 8011, 29, Rue Jeanne Marvig
31055 Toulouse, France
Dr. V. Viallet, Dr. V. Seznec, Dr. M. Morcrette, Prof. J.-M. Tarascon
Laboratoire de Réactivité et de Chimie des Solides (UMR 6007)
Université de Picardie Jules Verne
80039 Amiens, France
Dr. A. Aboulaich,[+] Dr. R. Bouchet, Dr. L. Tortet
Laboratoire MADIREL
Université d'Aix Marseille I, II, III-CNRS (UMR 7246)
Centre Saint Jérôme
13397 Marseille Cedex 20, France
E-mail: Renaud.Bouchet@univ-amu.fr
[+] Present address: Centre de recherche REMINEX, Groupe MANAGEM, Site de Hajar, BP469, Marrakech medina, Marrakech, Maroc

DOI: 10.1002/adfm.201102479

to assemble laminated ceramics (composite anode/electrolyte/composite cathode) in such a way that intimate interfaces can be generated, both between the solid grains of the materials in each of the three parts, and between the components themselves. It is often very difficult to sinter such a stacking of different materials sufficiently, because the different layers generally require different optimal sintering temperatures and present different thermal expansion coefficients, which may lead to the formation of cracks and delamination at the interfaces. In this perspective, this paper proposes an original methodology to design and optimize multifunctional ceramics, allowing the building of a safe, self-supported monolithic battery with a high surface energy by addressing the key critical point of making a "piece of stone" that is able to store electrical energy reversibly. First of all, the development of bulk-type, all-solid-state batteries requires the material selection to be based not only on electrochemical criteria to ensure a high performance, but also on criteria linked to the sintering process, like the thermal properties and chemical compatibilities. To show the feasibility of thick, all-solid-state batteries (surface capacities higher than a few mA h cm^{-2} and electrode thicknesses higher than 200 µm), two phosphate compounds were selected on the basis of their high stability upon sintering, as recently confirmed.[12,13] The sodium superionic conductor (Nasicon) ceramic, $Li_{1.5}Al_{0.5}Ge_{1.5}(PO_4)_3$ (LAG), was chosen as the solid electrolyte, as it offers a high ionic conductivity (3×10^{-4} S cm^{-1} at 25 °C with a Li^+-transport number of 1) and an excellent stability at potentials up to 7 V.[14] However, at low potential, the germanium is reduced in the presence of Li^+ ions to form Li_xGe intermetallic compounds, destroying the Nasicon structure, which implies a careful selection of the negative electrode.[15] Monoclinic $Li_3V_2(PO_4)_3$ (LVP) was chosen as both the negative- and positive electrode material in order to build symmetric composite-LVP/LAG/composite-LVP batteries. LVP presents a reversible capacity of 80 mA h g^{-1} at 1.8 V versus Li^+/Li (corresponding to insertion/deinsertion of 1.2 Li^+ ions per mole of LVP) within the stability window of the LAG solid electrolyte. As a positive electrode, it presents reversible capacities of 120 mA h g^{-1} between 3 and 4.2 V, and 140 mA h g^{-1} between 3 and 4.65 V, versus Li^+/Li. [16]

As shown recently, monolithic, all-solid-state batteries can be obtained in a few minutes using the spark plasma sintering (SPS) technique to sinter the composite electrodes and the electrolyte simultaneously.[17] Such an approach has allowed the assembly of battery prototypes that were cycled at least 30 times with only a small capacity fading, demonstrating the possibility of developing a viable, thick, solid-state technology. With regard to this result, the present paper is aimed at understanding the reasons for this interesting behaviour. The assembly of symmetric LVP/LAG/LVP batteries by SPS is addressed specifically, and the optimization of the composite-electrode formulation (LVP/LAG/carbon) is highlighted. Considering different materials (electrode and electrolyte materials), the principal challenge was first to produce a multimaterial stack composed of two, thick, composite ceramic electrodes, separated by an ionic conducting ceramic, with the whole structure being able to withstand the mechanical stresses induced by the volume changes of the active material during lithium intercalation and deintercalation. Then, regarding the electrochemical concerns, the principal limitation comes from charge transport through the electrolyte and the composite electrodes. Therefore, we show how the electrical properties (ionic and electronic) can be used as a tool to guide the optimization of the formulation of the electrode, the microstructure of the ceramics and, consequently, the sintering process conditions, while preserving a good mechanical stability. The optimized electrode formulation and sintering protocol was then used to assemble battery prototypes in one step, which were cycled at 80 °C.

2. Results and Discussion

2.1. Structure of Initial Powders and Processed Ceramics

The LAG and LVP starting powders were formed by agglomerates with rather inhomogeneous sizes (<50 µm) (**Figure 1**a,d). At higher magnification, these agglomerates were found to consist of primary rectangular particles, in the case of LAG material, and ovoid particles, in the case of LVP material; both had particles sizes of around 1–2 µm (Figure 1b,e). The microstructures of the dense LAG and LVP ceramics processed by SPS (680 °C, 100 MPa, 2 min) are presented respectively in Figure 1c,f. The LAG ceramic shows a limited grain growth, due to the fast heat treatment (Figure 1c), as well as less porosity in comparison with the LVP ceramic (Figure 1f).

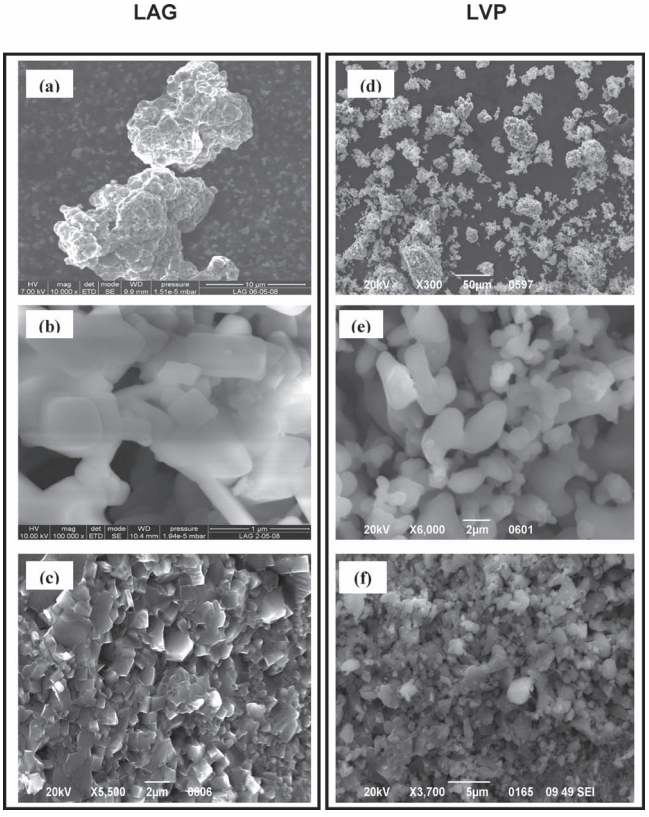

Figure 1. a–f) SEM images of the initial LAG powder (a,b), the LAG ceramic processed by SPS (c), the initial LVP powder (d,e), and the LVP ceramic processed by SPS (f) (SPS sintering parameters: 680 °C, 100 MPa, 2 min dwell time).

2.2. Electrical Properties of the Materials

2.2.1. LAG Electrolyte

Different sintering temperatures from 500 °C to 850 °C during the SPS experiments (75 MPa or 100 MPa and 2 min dwell time) were used to obtain LAG ceramics, leading to different compactnesses, from 57% to 93%, as shown in **Figure 2**a (the compactness being dimensionless and defined as the ratio of the experimental density to the theoretical density).

At high frequencies, the impedance spectrum, in Nyquist coordinates, (Figure 2b) was composed of two loops; the first one, at the highest frequencies, is related to the grains and the second to the grain boundaries. The sum of these two contributions gives the effective resistance of the sample. The effective conductivity of the LAG ceramic was calculated using the geometric parameters of the ceramics. The evolution of the LAG-ceramic conductivity as a function of temperature for different compactnesses is given in Figure 2c. The activation energy calculated from the slope of the curves is close to 0.39 eV and independent of the compactness, contrary to the conductivity, which increases with the compactness. From the isothermal variation of the conductivity as a function of the LAG compactness at 20 °C (Figure 2d), the value of the conductivity of a 100% dense LAG ceramic was extrapolated to 2.8×10^{-4} S cm^{-1}. Both values are in good agreement with the literature.[14] However, the impact of the electrolyte compactness is very important, since a drop by a factor of 6.4 for each loss of 10% of compactness was obtained. The modelling of this effect with a brick layer model, presented in a forthcoming paper, indicates that a compactness of at least 80% is necessary to reach a conductivity of 10^{-5} S cm^{-1}. As this value is the minimum to guarantee good electrochemical properties at moderate temperatures, the minimal sintering temperature should be set to 650 °C.

2.2.2. LVP Active Material

Following the same procedure, different SPS sintering protocols were applied for the preparation of LVP ceramics, for which the compactnesses were ≈70% at 680 °C (100 MPa, 2 min dwell time) and ≈75% at 750 °C (100 MPa, 2 min dwell time).

The characteristic impedance spectrum obtained at 130 °C from an LVP ceramic with a compactness of 76% is given in Figure 2e in Nyquist coordinates. A semicircle can be observed at high frequencies, which can be attributed to the LVP ceramic resistance; then, there is a small, flat contribution at medium frequencies, which may correspond to interfacial electron charge transfer and, finally, at low frequencies, the beginning of a loop that starts with a straight line, with a characteristic angle approaching 45° with the real axis can be seen. This last contribution is due to a diffusion process inside the LVP. In the case of a pure ionic conductor (even in the case of a mixed anion and cation conductor), the gold electrodes return a vertical straight line (capacitive effect see Figure 2b) at low frequencies, which is characteristic of ion-blocking electrodes. On the contrary, for a pure electronic conductor, the low frequency part is only a single point on the real axis, corresponding to the electronic resistivity. Thus, the impedance spectra suggest that the LVP ceramic is a mixed ionic/electronic conductor with charge-transport numbers for ions and electrons in the same range (these results were confirmed by DC measurements that are not shown here). From an Arrhenius plot of the conductivity as a function of temperature, an activation energy of 0.59 eV was obtained, and the effective conductivity above 80 °C was higher than 10^{-5} S cm^{-1}.

2.3. Composite Electrodes

The optimization of the electrode formulation is based on a compromise of several parameters, the two main ones being:

1 The composite electrode must present a good ionic and electronic percolation to ensure transport of ionic species and electrons. The electrode composition (LVP/LAG/C) is therefore critical.
2 The compactness of the composite electrode (and the all-solid-state battery) has to be high enough to ensure a good mechanical handling, as well as ionic/electronic percolation, while preserving enough "free space" to compensate the appearance of mechanical strains inside the composite electrode and to preserve the interfaces.

Therefore, with regard to these considerations, the sintering protocol has to be adjusted, while ensuring that no decomposition or reaction between the LAG, LVP and carbon occurs upon heat treatment.

These different points were thus considered, starting with the chemical compatibilities between the different materials during the sintering process. X-ray diffraction (XRD) analysis (**Figure 3**) of composite electrodes sintered by SPS at different temperatures showed that no reaction occurred at temperatures up to 680 °C (100 MPa/2 min dwelling time). This temperature was then set as the maximum to obtain composite electrodes.

With the electronic conductivity within the composite electrode being mainly ensured by the amount of carbon (Csp), the electrical behaviour of composite electrodes with 5, 10 and 15 wt% (8, 15, 23 vol%, respectively) of carbon was investigated in a 1/1 LVP/LAG-ratio formulation. The results reported in **Figure 4**a show that, to reach values higher than 1 S cm^{-1}, at least 10 wt% of Csp was necessary. Then, for a constant ratio of carbon (10 wt%), the influence of the LVP/LAG ratio (1/2, 1/1 and 2/1) was also scrutinized. The results obtained for composites with formulations 30LVP/60LAG/10C, 45LVP/45LAG/10C and 60LVP/30LAG/10C (in wt%) show that the electronic conductivity was increased with the decrease of the LVP/LAG ratio. The combination of the two results leads to the optimal formulation of 25LVP/60LAG/15C (wt%) to be defined.

Figure 4b shows the compactness as a function of the sintering parameters for two electrode formulations. The compactness of the composite electrode for similar sintering parameters (680 °C, 100 MPa, 2 min dwell time) was higher in the case of the 25LVP/60LAG/15C electrode composition (compactness of 86%) in comparison with the 45LVP/45LAG/10C electrode composition (compactness of 70%). As observed, the compactness of the composite electrodes, as well as the electronic conductivity, increased systematically when the amount of LAG increased.

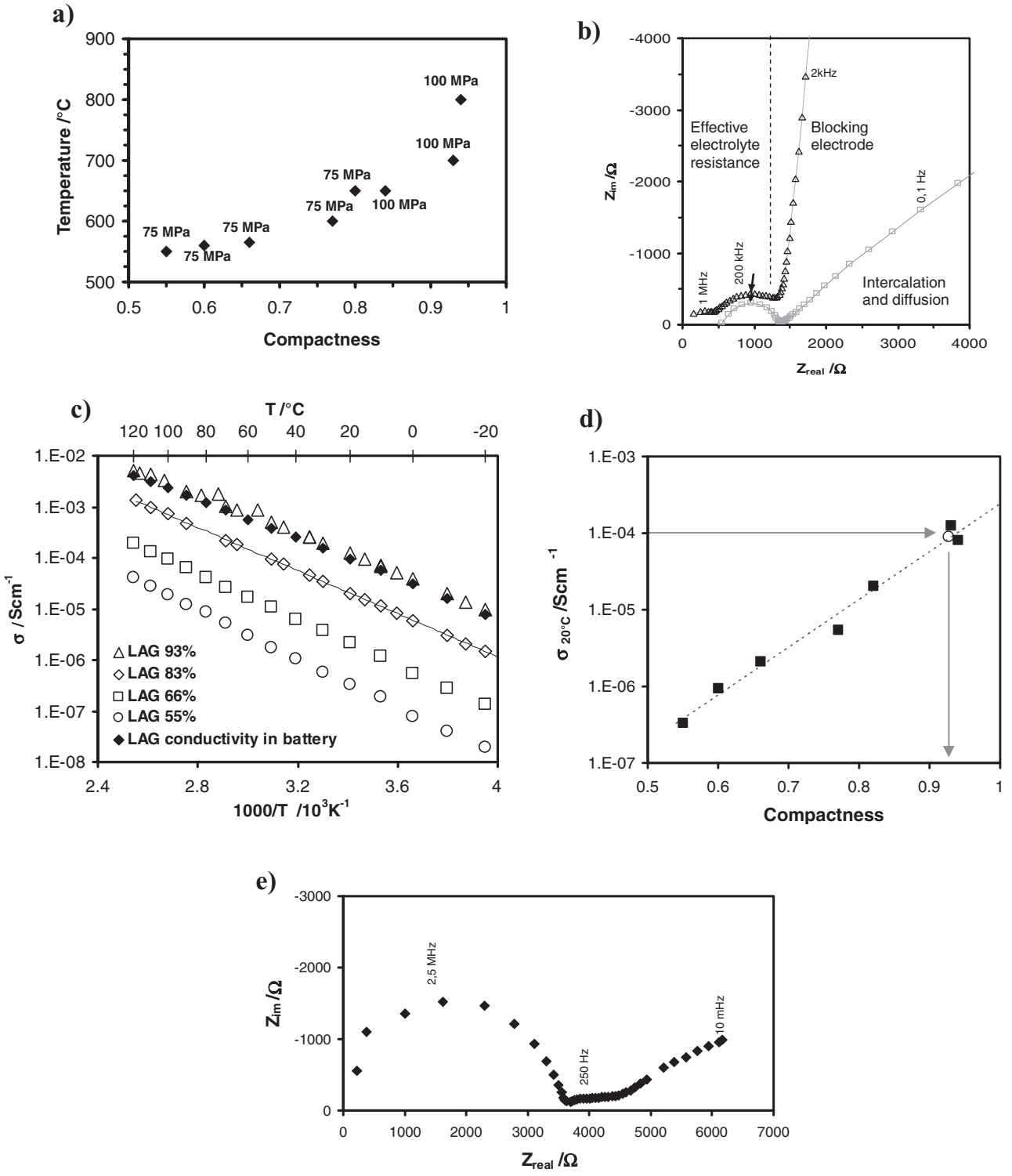

Figure 2. a) Influence of the sintering temperature and pressure (constant dwell time of 2 min) on the compactness of the LAG electrolyte ceramics. b) Electrochemical impedance diagram obtained at room temperature for the thick, solid-state lithium-ion battery LVP/LAG/LVP (open squares), and the LAG electrolyte (open triangles) sintered by the SPS technique. c) Temperature dependence of the ionic conductivity of LAG ceramics with different compactnesses (open symbols). d) Isothermal variations of the effective conductivity of the LAG ceramics as a function of compactness. This curve was used as a reference graph to obtain the "electrical" compactness of the LAG electrolyte in battery prototypes directly (open circles). e) Characteristic impedance spectrum of gold-metallized LVP ceramics with a compactness of 76% at 130 °C. Some of the characteristic frequencies are indicated.

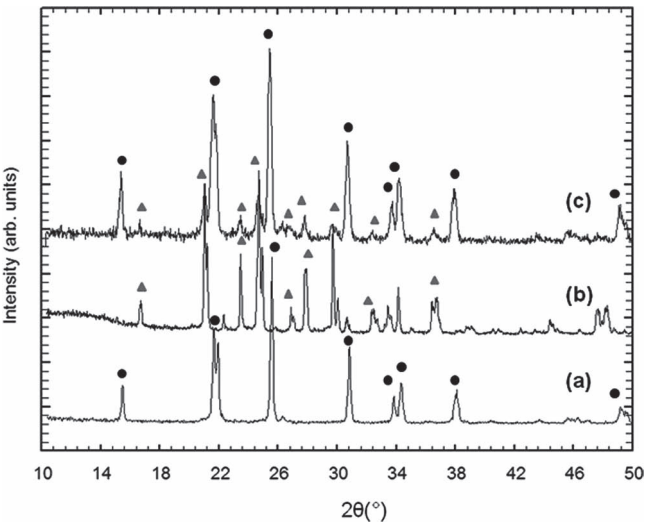

Figure 3. XRD diffractograms of the starting LAG powder (a), the starting LVP powder (b), and the composite electrode (LVP/LAG/Csp) processed by SPS (680 °C, 100MPa and 2 min dwelling time) (c).

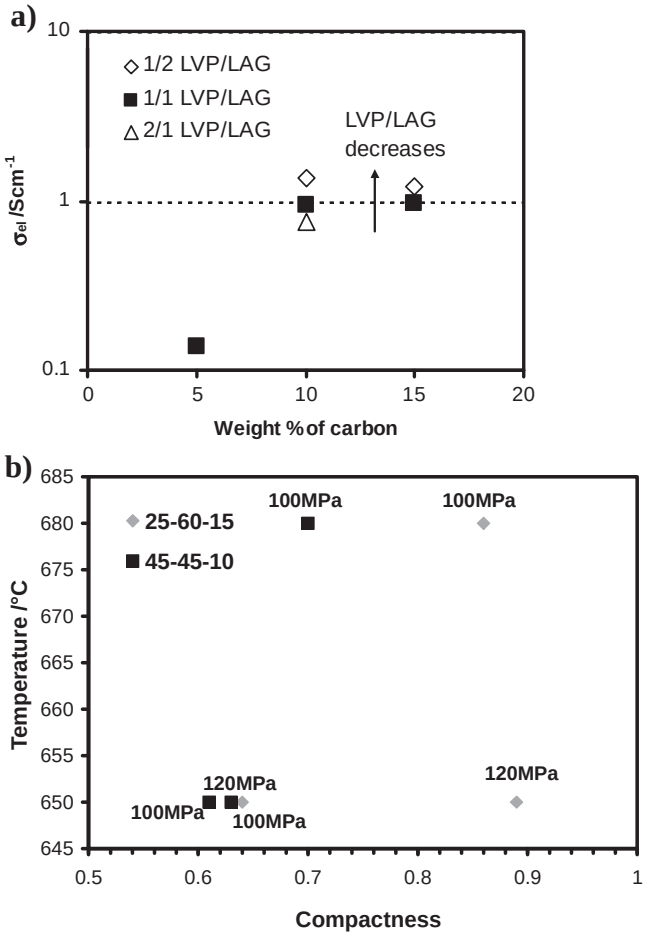

Figure 4. a) Electronic percolation of LVP/LAG/Csp composite electrodes sintered with the optimized SPS conditions. b) Influence of the SPS sintering temperature and pressure (constant dwell time of 2 min) on the compactness of composite electrodes (LVP/LAG/Csp) with different formulations.

To understand this result, the microstructures of processed ceramics with LVP/LAG ratios of 1/2, 1/1 and 2/1, and 10 wt% of carbon, were analyzed. The pellet microstructures corresponding to LVP/LAG ratios equal to 1/2 or 1/1 (**Figure 5**a,b) were quite similar and were made of large (10 to 20 μm), dense electrolyte regions surrounded by porous regions composed of smaller LAG and LVP grains covered by carbon (black regions in Figure 5), which ensure electronic percolation. The compactness of the LAG and LVP pellets after sintering at 680 °C (100 MPa/2 min dwell time) were, respectively, 84% and 70%. This clearly indicates that the LAG electrolyte was sintered before the active material and acts as cement in the composite electrodes, ensuring both mechanical integrity and ion transport in the electrode. During the sintering of the LAG, the LVP and carbon were segregated in the porosity of the LAG network (Figure 5a (zoom) and d). Therefore, the LVP grains were found to be surrounded by carbon beads with many connections to the LAG network. This local environment of the LVP appears to be an important key for the relaxation of the interfacial stress during electrochemical cycling. The microstructure of the composite electrode with an LVP/LAG ratio equal to 2/1 was, as expected, more porous for similar sintering parameters, as shown in Figure 5c. It was mainly constituted of small LVP grains surrounded by a porous network of carbon and isolated LAG grains. It is also noteworthy that the increase of the electronic conductivity as the amount of LAG increased is consistent with literature relating to inorganic solid-state electrodes thicker than a few micrometers.[18–23] The formulation of the composite electrodes to ensure ionic and electronic percolation within the electrode volume lies generally in the range of 25–30% of active materials and 55–65% of electrolyte, with the rest being the electronic conductor (10–20%). However, the intrinsic electrical properties of the active material are very important, as was the case for olivine-type active materials, which are very poor electronic conductors and thus need a carbon coating to deliver their energy.[24] According to our data, LVP is a mixed ionic/electronic material, which may assist electron and ion charge transport through the volume of the composite electrode. Finally, a higher amount of active material could be obtained in the formulation notably by playing on the electrolyte grain size and improving the mixing of the precursor powders, allowing both the homogenization of the chemical compound distribution into the bulk of the electrode, and, therefore, the efficiency of electronic and ionic percolation, to be improved.

As a summary of the criteria deduced from these studies, it appears that to sinter the composite electrode and then the battery, the temperature should be selected to sinter the electrolyte (LAG) fully, in order that it forms a continuous network in the composite electrodes, ensuring both the mechanical framework and ion transport in the whole battery. According to the microstructure of the starting powders, the optimized formulation contains at least 10 wt% of Csp and an LVP/LAG ratio close to 1/2. A composite electrode compactness of around 85% seems to be a good compromise, allowing good mechanical handling, as well as good electronic percolation. Furthermore, the residual porosity and local composite architecture allows the connection of LAG and LVP grains only at some localized points (Figure 5d), allowing the "structure" to move and dissipate mechanical constraints as the ionic species will insert into and be removed from the LVP structure during cycling.

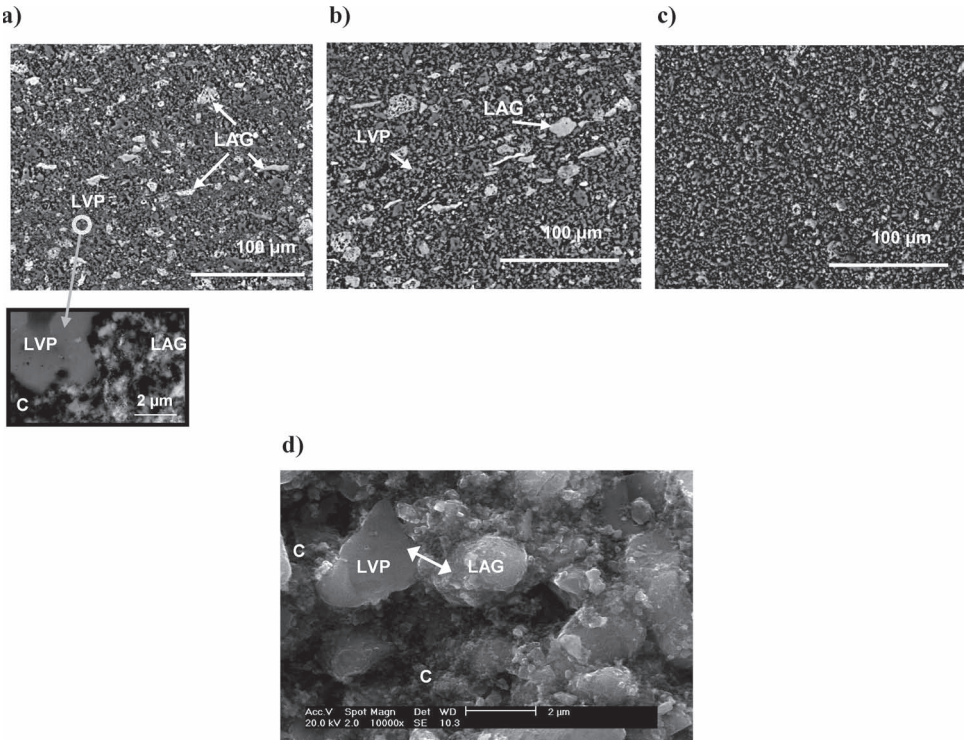

Figure 5. a–c) Back-scattered electron images of the polished ceramics processed by SPS (680 °C, 100 MPa, 2 min dwell time). LVP/LAG ratios (10 wt% C): 1/2(a), 1/1 (b), and 2/1(c). d) SEM photograph of a broken LVP/LAG/Csp (25/60/15) composite electrode sintered by SPS (680 °C, 100 MPa, 2 min dwell time).

2.4. Battery Assembly

Based on our results, the optimized composite electrode formulation (25LVP/60LAG/15Csp (wt%)) and the optimized sintering parameters (680 °C, 100MPa, 2 min dwell time) were used to build a symmetric prototype with a positive-electrode/negative-electrode mass ratio close to unity. **Figure 6**a shows a picture of one all-solid-state battery prototype, assembled by SPS. Figure 6b demonstrates the good mechanical properties of this all-ceramic bulk-type battery, which has clean and well-defined interfaces (Figure 6c).

The electrical properties of the battery, measured by impedance spectroscopy (Figure 2b), were used to deduce the compactness of the electrolyte between the two composite electrodes using Figure 2d as a reference graph. A compactness of 92% was deduced based on the measured ionic conductivity (red arrows in Figure 3d), which is in good agreement with the geometrical estimation. The composite electrode's compactness of about 80–85%, as expected, was lower than the compactnesses of pure LVP and pure LAG pellets, about 70% and 84%, respectively, at 680 °C. The electrode and electrolyte thicknesses were all around 400 µm.

The galvanostatic cycling of the prototype at 80 °C, at rates of C/50 or C/25, is shown in Figure 6d. The results show good cycling performances with surface capacities of 1, 2 and 2.2 mA h cm^{-2}, depending on the selected cut-off voltage, for 1.75, 2.35 or 2.45 V, respectively.

3. Conclusions

This work provides a new path worth pursuing for the design of inorganic Li-ion batteries capable of operating completely safely over a wide temperature range, and with a surface capacity comparable to that of classical lithium-ion batteries. To design efficient, monolithic, all-solid-state batteries, several parameters need to be considered: the choice of materials, the granulometry of the starting powder, the composite electrode formulation, and the sintering conditions affect the ionic and electronic percolation paths through the volume of the composite electrode and thus the electrochemical performance. The optimization of the composite electrodes requires the correlation of their microstructure with their electrical properties. Finally, a solid-state battery prototype was assembled by SPS considering the optimized parameters. The first results show good cycling and a promising electrochemical performance (surface capacity of ≈2.2 mA h cm^{-2} with a cut-off voltage of 2.45 V). The local architecture of the composite electrode is believed to be a key parameter, allowing stress relaxation during cycling.

4. Experimental Section

Materials: The active material, A-$Li_3V_2(PO_4)_3$ (LVP) powder, was obtained by initial homogenization of the precursors (stoichiometric amounts of NH_4VO_3 and LiH_2PO_4) dissolved in an aqueous solution (1 mol L^{-1}), followed by the slow evaporation of H_2O at 100 °C and that

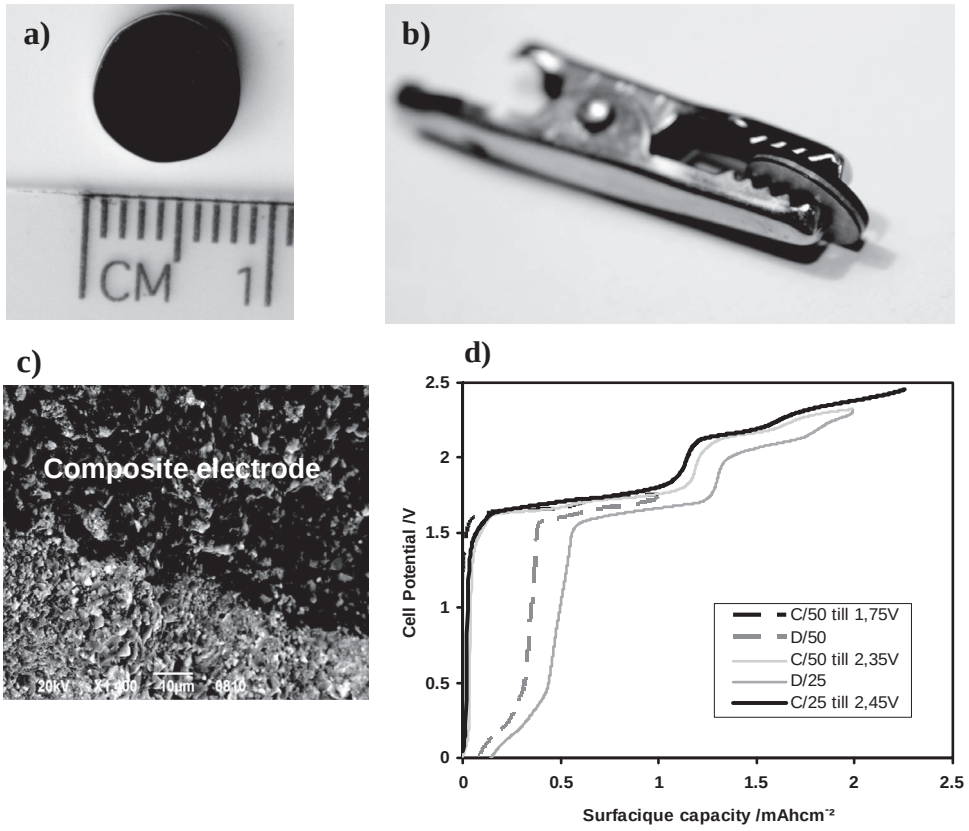

Figure 6. a–b) Pictures of an LVP/LAG/LVP battery obtained by the SPS technique. c) SEM image of the interface electrolyte/composite electrode in a broken solid-state battery (SPS sintering parameters: 680 °C, 100 MPa, 2 min dwell time). d) Charge/discharge profiles obtained at 80 °C and C/50 or C/25 for one symmetrical LVP/LAG/LVP battery prototype (electrode composite composition: 25LVP/60LAG/15Csp)

of volatile species at 400 °C under Ar/H_2. Then, a second annealing was conducted at 750 °C (12 h) under Ar/H_2 gas flow (10%) to achieve reduction of V (V) to V (III).[16]

The solid electrolyte, $Li_{1.5}Al_{0.5}Ge_{1.5}(PO_4)_3$ (LAG), was synthesized as follows. Germanium and aluminum alkoxide reactants, $Ge(OC_2H_5)_4$ and $Al(OC_4H_9)_3$, were dissolved in tetrahydrofuran (THF) and lithium and ammonium salts (pure $CH_3COOLi{\bullet}2H_2O$ and pure $NH_4H_2PO_4$) were dissolved in water. After dissolution of the precursors, the water solution was added drop by drop to the alkoxide solution. Then, the excess of solvent was removed by heating at 80 °C while stirring the solution, and an appropriate heat treatment (2 h at 850 °C) was performed to generate the pure phase with a well-controlled microstructure.

Carbon black (Csp) (Ketjen Black from Timcal) was used as the additive that imparts electronic conductivity to the solid-state composite electrode.

Sintering of the Composite Electrodes, the Electrolyte, and the Battery Assembly by Spark Plasma Sintering: The pellets were obtained in 10 min thanks to the use of the SPS technique. Prior to the one-step battery assembly, different thermomechanical cycles for the SPS were tested on the electrolyte (the LAG or the active material (LVP) alone, and the composite electrodes (LVP/LAG/C)), leading to ceramics with different compactnesses.

The composite electrodes were prepared by the hand mixing of the LVP, LAG and Csp. The same formulation was used for the negative and positive electrodes, and the battery was assembled under vacuum by SPS in a graphite die with an inner diameter of 8 mm. Typically, the battery prototypes had a diameter of 8 mm and a thickness of about 1.2 mm.

Microstructure, Impedance Spectroscopy, and Electrochemical Measurements: The microstructures of the starting powders (LVP, LAG) and those of the ceramics processed by SPS (electrolyte LAG alone, active material LVP alone and LVP/LAG/C composite electrode) were analysed using scanning electron microscopy (SEM) (FEG, LEO 1530).

XRD was performed using a D8 Bruker instrument in the range 10–50° (2θ), using Cu K_α radiation.

The conductivities of the LVP and LAG starting materials and of the composite electrodes were characterized in the temperature range 30–130 °C using electrochemical impedance spectroscopy (Solartron 1260) in the frequency range from 1 mHz to 10 MHz, with an excitation voltage of 20 mV. Thin gold layers were deposited by physical vapor deposition (PVD) on each face of the ceramics obtained by SPS as (ion-) blocking electrodes. Then, the metallized ceramics were dried over 5 d in a glove box (H_2O < 3 ppm), before being mounted in tightened swagelock type cells to perform the electrochemical measurements outside the glove box. The impedance data were modelled using the Z-View software (Scribner inc.). Finally, the electrochemical performance of one battery prototype was determined at 80 °C and at a current density ranging from 40 μA cm^{-2} (C/50, C/1 or C being defined as one Li^+ (resp. 1 electron) exchanged in 1 h) to 80 μA cm^{-2} (C/25), using a battery-test device (Solartron 1470).

Acknowledgements

The authors express their sincere gratitude to the French National Research Agency (Project CeraLion-ANR-07-Stock-E-04) and the Aerospace Valley competitiveness cluster for their financial support.

Received: October 14, 2011
Published online: February 22, 2012

[1] A. Hammami, N. Raymond, M. Armand, *Nature* **2003**, *424*, 635.
[2] J. B. Goodenough, Y. Kim, *Chem. Mater.* **2010**, *22*, 587.
[3] K. Murata, S. Izuchi, Y. Yoshihisa, *Electrochim. Acta* **2000**, *45*, 1501.
[4] N. J. Dudney, *Mater. Sci. Eng. B* **2005**, *116*, 245.
[5] A. Levasseur, M. Menetrier, R. Dormoy, G. Meunier, *Mater. Sci. Eng. B* **1989**, *3*, 5.
[6] H. Ohtsuka, J. Yamaki, *Jpn. J. Appl. Phys.* **1989**, *28*, 2264.
[7] H. Ohtsuka, S. Okada, J. Yamaki, *Solid State Ionics* **1990**, *40*, 964.
[8] M. Baba, N. Kumagai, H. Kobayashi, O. Nakano, K. Nishidate, *Electrochem. Solid-State Lett.* **1999**, *2*, 320.
[9] F. Kirino, Y. Ito, K. Miyauchi, T. Kudo, *Nippon Kagaku Kaishi* **1986**, *3*, 445.
[10] K. Kanehori, K. Matsumoto, K. Miyauchi, T. Kudo, *Solid State Ionics* **1983**, *9–10*, 1445.
[11] A. Patil, V. Patil, D. W. Shin, J.-W. Choi, D.-S. Paik, S.-J. Yoon, *Mater. Res. Bull.* **2008**, *43*, 1913.
[12] J. Xie, N. Imanishi, T. Zhang, A. Hirano, Y. Takeda, O. Yamamoto, *J. Power Sources* **2009**, *189*, 365.
[13] E. Kobayashi, L. S Plashnitsa, T. Doi, S. Okada, J.-I. Yamaki, *Electrochem. Commun.* **2010**, *10*, 892.
[14] M. Crétin, P. Fabry, *J. Eur. Ceram. Soc.* **1999**, *19*, 2931.
[15] J. K. Feng, L. Lu, M. O. Lai, *J. Alloys Compd.* **2010**, *501*, 255.
[16] S. Patoux, C. Wurm, M. Morcrette, G. Rousse, C. Masquelier, *J. Power Sources* **2003**, *119–121*, 278.
[17] A. Aboulaich, R. Bouchet, G. Delaizir, V. Seznec, L. Tortet, M. Morcrette, P. Rozier, J.-M. Tarascon, V. Viallet, M. Dollé, *Adv. Energy Mater.* **2011**, *1*, 179.
[18] A. Sakuda, H. Kitaura, A. Hayashi, K. Tadanaga, M. Tatsumisago, *J. Power Sources* **2009**, *189*, 527.
[19] A. Hayashi, T. Ohtomo, F. Mizuno, K. Tadanaga, M. Tatsumisago, *Electrochem. Commun.* **2003**, *5*, 701.
[20] F. Mizuno, A. Hayashi, K. Tadanaga, T. Minami, M. Tatsumisago, *J. Power Sources* **2003**, *124*, 170.
[21] F. Mizuno, A. Hayashi, K. Tadanaga, T. Minami, M. Tatsumisago, *Solid State Ionics* **2004**, *175*, 699.
[22] A. Hayashi, T. Konishi, K. Tadanaga, M. Tatsumisago, *Solid State Ionics* **2006**, *177*, 2737.
[23] M. Tatsumisago, F. Mizuno, A. Hayashi, *J. Power Sources* **2006**, *159*, 193.
[24] J.-C. Delacourt, L. Laffont, R. Bouchet, C. Wurm, J.-B. Leriche, M. Mocrette, J.-M. Tarascon, C. Masquelier, *J. Electrochem. Soc.* **2005**, *152*, A913.